Microsc. Microanal. 15, 99–105, 2009
doi:10.1017/S1431927609090199

Microscopy AND Microanalysis

X-Ray Microanalysis Combined with Monte Carlo Simulation for the Analysis of Layered Thin Films: The Case of Carbon Contamination

Aldo Armigliato[1,*] and Rodolfo Rosa[1,2]

[1]*CNR-IMM, Sezione di Bologna, Via P. Gobetti 101, 40129 Bologna, Italy*
[2]*Università di Bologna, Dipartimento di Scienze Statistiche, Via delle Belle Arti, 41, 40126 Bologna, Italy*

Abstract: A previously developed Monte Carlo code has been extended to the X-ray microanalysis in a (scanning) transmission electron microscope of plan sections, consisting of bilayers and triple layers. To test the validity of this method for quantification purposes, a commercially available NiO_x ($x \sim 1$) thin film, deposited on a carbon layer, has been chosen. The composition and thickness of the NiO film and the thickness of the C support layer are obtained by fitting to the three X-ray intensity ratios $I(\mathrm{NiK})/I(\mathrm{OK})$, $I(\mathrm{NiK})/I(\mathrm{CK})$, and $I(\mathrm{OK})/I(\mathrm{CK})$. Moreover, it has been investigated to what extent the resulting film composition is affected by the presence of a contaminating carbon film at the sample surface. To this end, the sample has been analyzed both in the (recommended) "grid downward" geometry and in the upside/down ("grid upward") situation. It is found that a carbon contaminating film of few tens of nanometers must be assumed in both cases, in addition to the C support film. Consequently, assuming the proper $C/NiO_x/C$ stack in the simulations, the Monte Carlo method yields the correct oxygen concentration and thickness of the NiO_x film.

Key words: analytical electron microscopy, Monte Carlo simulation, nickel-oxide films, bilayers

Introduction

Thin film X-ray microanalysis is often performed by depositing the layer containing the material of interest onto an amorphous carbon film, supported by an electron microscopy grid. Quantification of the concentration of the various elements in the film is in principle possible, provided carbon is not included among them. A number of methods for transmission electron microscopes (TEM), equipped with energy dispersive spectrometers (EDS), is available, but, to our knowledge, none of them can analyze a bilayer in a way similar to the case of a multilayer deposited on a bulk substrate (see, e.g., the PAP software by Pouchou & Pichoir, 1991, frequently applied to microanalysis experiments in the scanning electron microscope). The feasibility of quantitative X-ray microanalysis of a stack of two and more layers in TEM applications would also be desirable. The popular Cliff-Lorimer approach (Cliff & Lorimer, 1975) yields the film composition from properly determined *k*-factors only when the so-called "thin film approximation" holds, otherwise the X-ray absorption correction must be calculated, which requires an independent measurement of the film thickness. In such cases, when absorption is significant, as in the case of the OK X-ray line in the NiO film investigated in this article, the extrapolation technique by Horita et al. (1986) has proved to be useful. Westwood et al. (1992) applied it successfully to determine the Cliff-Lorimer *k*-factors at zero foil thickness in standards used for the analysis of oxygen segregation in aluminum nitride. Other proposed schemes can determine both film thickness and composition, but again of a single layer (Horita et al., 1989; Watanabe & Williams, 2006). Consequently, it is generally accepted that a carbon film placed between the film of interest and the grid has scarce influence on the quantification and is thus ignored. It is just recommended that the sample be mounted in the microscope with the grid downward (away from the electron beam).

The aim of this work is to demonstrate that, in the case of films containing light elements, as for the presently investigated NiO film, the presence of a carbon *overlayer*, due to contamination, can be included into the quantification procedure of our Monte Carlo code (Rosa & Armigliato, 1989; Armigliato & Rosa, 1990; Armigliato, 1999), yielding correct film composition values. This is accomplished by using the intensity ratios of the X-ray peaks generated by the Ni, O, and C in the specimen. It is worthwhile noting that, when the sample consists of a stack of two or three layers, as in the present case of a C(contamination)/NiO/C(support) vertical sequence, the Monte Carlo method outperforms other analytical approaches, which are applicable only when

Received November 27, 2008; accepted January 5, 2009.
*Corresponding author. E-mail: armigliato@bo.imm.cnr.it

every additional layer to the film under investigation can be ignored.

Materials and Methods

The NiO/C test specimen proposed by Egerton and Cheng (1994) for the characterization of analytical electron microscopes has been employed in our experiments. It is commercially available from Emitech Ltd (NiOX^{TM}, http://www.emitech.co.uk) and consists of a thin film of NiO_x ($x \sim 1$), deposited onto amorphous carbon and supported by a 200-mesh molybdenum grid. The relevant thickness values for our specific sample (batch D) are 55 nm for the NiO_x film and 20 nm for the carbon layer. According to Egerton and Cheng (1994), the O/Ni atomic ratios of these standards range from 0.92 to 1.02. A similar specimen has been analyzed by the so-called ζ-factor method (Watanabe & Williams, 2006) with good results.

Prior to its insertion into the microscope, the specimen was plasma cleaned for 2 min by a Fischione instrument (Model 1020) to remove surfacial hydrocarbon contamination.

A 200 kV FEI Tecnai F20 FEG-(S)TEM, equipped with a high-angle annular dark-field (HAADF) detector, the TIA (Tecnai Interface Analysis) software, and an EDAX Sapphire detector was employed for X-ray microanalysis of the NiO/C sample. The acquisition of X-ray spectra in a region of the specimen was performed by 10-point linescans, using an electron spot of about 1 nm in diameter. Three different tilt angles toward the detector have been used: 10°, 15°, and 20° that correspond to the take-off angles of 24.7°, 29.7°, and 34.7°, respectively, as the elevation angle of the spectrometer is 14.7°.

Because of the need for analyzing, in addition to the NiO film, also the 20 nm thick amorphous carbon layer, and to minimize carbon contamination, the sample temperature was kept at 100 K during the analysis, by using a Gatan LN_2-cooled double-tilting holder. The scanning transmission electron microscope (STEM) cold finger was also used to further reduce sample contamination.

Results

Figure 1 shows a sketch of the investigated sample and two of its possible orientations with respect the incident electron beam of the STEM: grid downward (Fig. 1a) and grid upward (Fig. 1b). Accordingly, the C layer is below (a) or above (b) the NiO film, respectively. Although only the former is recommended, as the influence of the C support on the oxygen concentration is considered as negligible, mounting the sample upside down is useful for our Monte Carlo analysis of the bilayer. In addition, as it will be shown later on, the result of this test can be extended to the detection of a carbon contamination overlayer and to its effect on the NiO film quantification.

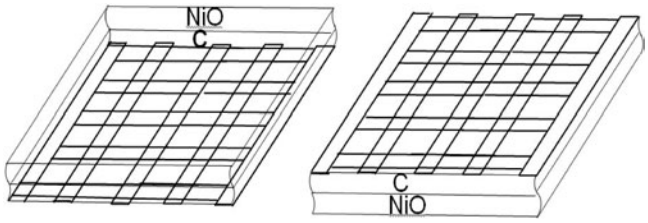

Figure 1. Sketch of the investigated NiO film, deposited on a C-coated Mo grid, to show the different loading in the microscope holder. (**a**) Grid (and C layer) below the NiO film (referred to in the text as "grid downward"); (**b**) grid above the NiO film ("grid upward"). Though this latter geometry is not recommended in normal quantitative analysis, it has been analyzed by our Monte Carlo to determine the effect of a C-overlayer on the oxygen concentration in the NiO film (see text for details).

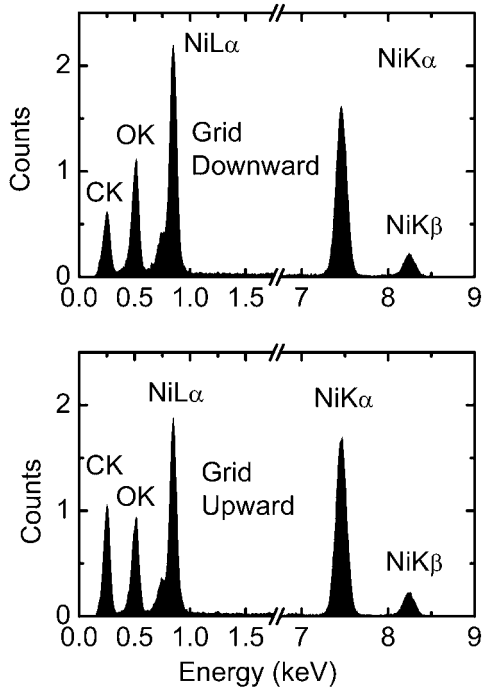

Figure 2. X-ray spectra taken with grid downward (top) and upward (bottom). Note the difference in the OK intensity in the two spectra, as compared with the NiK one, despite the small thickness of the carbon layer (20 nm). This is due to the strong absorption of the OK X-rays in carbon.

An example of spectra obtained in the two configurations, acquired for 60 s (livetime), is reported in Fig. 2. They refer to a tilt angle of 20° and correspond to the geometry of Figure 1a and Figure 1b, respectively. Because the height of the NiKα peak in these spectra is about the same, the difference between the CKα and OKα peak intensities is

Table 1. Values of Ionization Cross Sections Q, Fluorescence Yields ω, Detector Absorption ε, and Weight p of the Lines for the Three X-Ray Lines Generated by the Electron Beam in the NiO/C Sample*

	Q ($\times 10^{-20}$) cm^2				
Parameter	B-W	Powell	ω ($\times 10^{-3}$)	ε	p
CK	0.93	1.9	2.8	0.25	1
OK	0.45	0.92	8.3	0.51	1
NiK	0.017	0.029	406	0.997	0.88

*For Q, the values by Williams (1933), who corrected the Bethe (1930) formula for relativistic effects (B-W), are reported together with those by Powell (1976).

Table 2. Mass Absorption Coefficients for CKα, OKα, and NiKα in the NiO/C Bilayer, According to the Tabulation by Veigele (1973)

	Emitter μ/ρ (cm^2/g)		
Absorber	CKα	OKα	NiKα
Carbon	3,156	12,184	6
Oxygen	7,809	1,269	16
Nickel	19,689	5,243	67

clearly visible. From the net peak intensities, three ratios—$I(\text{NiK})/I(\text{OK})$, $I(\text{NiK})/I(\text{CK})$, and $I(\text{OK})/I(\text{CK})$—are obtained. These are the experimental data required as an input to our Monte Carlo code. To do this, up to six regions of interest (ROIs) are selected in an energy range from 0 to 10 keV of the experimental spectrum, all in areas not containing a peak; their width is 30 eV (e.g., between CK and OK, OK and NiL) and 1 keV elsewhere (three ROIs between NiL and NiKα, and one beyond NiKβ). Then the background is substracted according to the option called "empirical," available in the ESVision software by Emispec (http://www.emispec.com); it is an empirically refined Kramer's law model that includes corrections for detector absorption.

To convert the X-ray intensities into concentrations of the elements, it is necessary to know the values of fundamental parameters such as the ionization cross sections Q at 200 kV, the fluorescence yields ω, the mass absorption coefficients of the X-ray line of element i in the sample $(\mu/\rho)^i_{sample}$, the weight of the NiKα line, and the detector absorption ε.

We have considered three relativistic cross sections Q, namely the ones proposed by Williams (1933), who extended to relativistic electrons Bethe's (1930) equation, Powell (1976), and Egerton (1996), respectively. As the Egerton's Q values are very close to those calculated by Powell, we have reduced the choice to the two former tabulations [Bethe-Williams (henceforth called B-W) and Powell]. Moreover, the fluorescence yields ω tabulated by Krause (1979), the weight p of the lines (Schreiber & Wims, 1982), and the mass absorption coefficients by Veigele (1973) have been adopted. Finally, the ε values are obtained from the X-ray transmissivity to the various element lines of the 300 nm thick AP1.3 Moxtek window (http://www.moxtek.com/), placed in front of our EDAX Sapphire detector, as well as from that due to the silicon dead layer and the metal contact. These relevant data (Q, ω, and ε) are reported in Table 1, whereas the mass absorption coefficients for the elements present in the NiO/C bilayer are reported in Table 2. To compute the absorption correction, a density of 6.7 g/cm^3 has been assumed for the 55 nm NiO film: this is the value reported in both the standard's certificate and the literature. It must be noted that, due to the large absorption of OK in carbon, neglecting a carbon overlayer would lead to an incorrect NiO composition.

Monte Carlo Method

To estimate the O concentrations and the local film thickness, we have employed the so-called "2 tilt-angle" method, previously described in Armigliato and Rosa (1990) and Armigliato (1999). For the reader's convenience we recall briefly the Monte Carlo computer model and the "2 tilt-angle" method. The physical model (see Rosa & Armigliato, 1989 and references therein) adopts the single-scattering approach in which the angular deflection is determined by the elastic scattering and the energy loss between scattering points is given by the continuous slowing down approximation of the Bethe law. The Wentzel potential is employed to derive the cross section for elastic collisions. The relativistic Bethe stopping power has been adopted to describe energy dissipation by electrons in the target. The code can deal any film thickness in multilayer systems. When the path between two subsequent collisions crosses one or more boundary surfaces, the path is rescaled using the mean-free-path ratio in each layer.

The "2 tilt-angle" method yields simultaneously the composition and thickness of the thin film. It is based on the convergence of the data obtained by performing the analysis in different orientations of the sample.

Briefly, given a t thick binary film AB, the method consists of finding the values of C_A and t that minimize the difference between the experimental ratios of the measured X-ray intensities (R_{exp}) and the corresponding computed ratios (R_{calc}) for two tilt angles. This Monte Carlo method generates a table of R_{calc} values as a function of concentration C_A and local thickness t in a suitable range.

In the present case, we take as fixed the thickness of the C layer and minimize the difference $|R_{\text{exp}} - R_{\text{calc}}\,(C_{\text{O}}, t)|$, where $R = I(\text{OK})/I(\text{NiK})$. Taking into account all possible (i.e., 100) measured ratios from the two sets of intensities, we can associate confidence intervals with the point esti-

Table 3. Estimates and Associated Errors of O Concentration C_O (at.%) and Thickness t (nm) of the NiO Film, Obtained by the Monte Carlo "2 Tilt-Angle" Method, with the Angle Couples 10–20° and 15–20°*

	Grid Downward				Grid Upward			
Q cross section	B-W		Powell		B-W		Powell	
Tilt Angles	C_O (at.%)	t (nm)	C_O (at.%)	t (nm)	C_O (at.%)	t (nm)	C_O (at.%)	t (nm)
10–20°	50.5 ± 1.5	600 ± 200	54.3 ± 1.5	590 ± 200	53.5 ± 1.0	520 ± 100	56.1 ± 1.0	520 ± 90
15–20°	50.3 ± 1.3	430 ± 180	53.0 ± 1.2	520 ± 180	52.4 ± 1.0	620 ± 140	55.8 ± 1.0	610 ± 140

*The results refer to Bethe-Williams (B-W) and Powell cross section and to both "grid downward" and "grid upward" geometries.

Table 4. Estimates and Associated Errors of O Concentration C_O (at.%) and Thickness t (nm) of the NiO Film, Obtained by the Monte Carlo "2 Tilt-Angle" Method, with a t_C^* Thick Carbon Contaminating Film on the Sample Surface*

	Grid Downward				Grid Upward			
Q cross section	B-W		Powell		B-W		Powell	
	C_O (at.%)	t (nm)	C_O (at.%)	t (nm)	C_O (at.%)	t (nm)	C_O (at.%)	t (nm)
$t_C^* = 10$ nm								
10–20°	49.8 ± 1.3	510 ± 170	51.2 ± 1.2	640 ± 150	52.9 ± 1.7	380 ± 160	54.0 ± 1.1	650 ± 180
15–20°	50.1 ± 1.3	490 ± 180	51.3 ± 1.3	480 ± 180	52.2 ± 1.0	460 ± 100	53.4 ± 1.0	640 ± 140
$t_C^* = 20$ nm								
10–20°	49.0 ± 1.2	500 ± 180	50.6 ± 1.3	640 ± 100	49.8 ± 1.2	590 ± 160	52.1 ± 1.3	610 ± 160
15–20°	49.1 ± 1.1	440 ± 150	50.8 ± 1.2	470 ± 160	50.2 ± 1.0	540 ± 100	52.8 ± 1.0	540 ± 100
$t_C^* = 30$ nm								
10–20°	48.3 ± 1.4	520 ± 180	49.5 ± 1.3	580 ± 150	49.3 ± 1.2	450 ± 110	51.2 ± 1.4	610 ± 160
15–20°	48.2 ± 1.3	450 ± 190	49.5 ± 1.3	450 ± 190	49.0 ± 1.7	560 ± 190	51.1 ± 1.7	550 ± 190

*The results refer to Bethe-Williams (B-W) and Powell cross section and to both "grid downward" and "grid upward" geometries.

mates. In addition, we have chosen two couples of tilt angles, namely 10–20° and 15–20°: the former increases the differential X-ray absorption, whereas the latter reduces the possible shadowing effect due to specimen holder. From the results (Tables 3, 4), it is deduced that the oxygen concentrations are in close agreement each other.

First consider the "grid downward" geometry, i.e., with the 20 nm thick carbon layer underlying the 55 nm thick NiO_x film. We obtain the results reported in Table 3 (left). In the first column are the tilt angles; in the second, the resulting C_O concentrations; and in the third, the resulting NiO film thickness. The errors represent one-half of the 68% confidence intervals.

As noted in our previous articles, the uncertainty associated with the estimated local thickness is rather high, although the certified value is within the range, so we limit our consideration to the concentrations. It appears the C_O concentration is in agreement with the certified one only by using the B-W section. Such a result might suggest, at a first glance, that only the B-W section is correct; however, we find some inconsistencies if we consider the geometry with the "grid upward." In the latter case the results are those reported in Table 3 (right). No agreement is obtained with either of the cross sections. In other words in the "grid downward" geometry, we find an agreement with the certified C_O (at least with the B-W cross section), while this agreement is lost in the "grid upward" geometry.

To clarify the above inconsistency, one needs to consider not only a single intensity ratio $[I(\mathrm{OK})/I(\mathrm{NiK})]$, but all of them, that is, also OKα/CKα and NiKα/CKα. The Monte Carlo–generated intensities are chosen from the already available computed values, assuming, in a first instance, $C_O = C_{Ni} = 50$ at.% and $t(\mathrm{NiO}) = 55$ nm. A clear disagreement with the experimental data occurs (first Monte Carlo row ($t_C^* = 0$, see below) in Tables 5, 6). It is worthwhile to note that the same is true for the three tilt angles and a

Table 5. Experimental and Monte Carlo–Generated Intensity Ratios $I(\mathrm{OK})/I(\mathrm{NiK})$, $I(\mathrm{OK})/I(\mathrm{CK})$, and $I(\mathrm{NiK})/I(\mathrm{CK})$*

Q cross section	Grid Downward					
	B-W			Powell		
Intensity ratios	$\frac{I(\mathrm{OK})}{I(\mathrm{NiK})}$	$\frac{I(\mathrm{OK})}{I(\mathrm{CK})}$	$\frac{I(\mathrm{NiK})}{I(\mathrm{CK})}$	$\frac{I(\mathrm{OK})}{I(\mathrm{NiK})}$	$\frac{I(\mathrm{OK})}{I(\mathrm{CK})}$	$\frac{I(\mathrm{NiK})}{I(\mathrm{CK})}$
Experimental	0.309 ± 0.005	2.46 ± 0.06	8.0 ± 0.3	0.309 ± 0.005	2.46 ± 0.06	8.0 ± 0.3
Monte Carlo						
$t_C^* = 0$ nm	0.30	10.33	34.47	0.35	10.33	29.57
$t_C^* = 10$ nm	0.29	3.91	13.74	0.33	3.91	11.79
$t_C^* = 20$ nm	0.27	2.33	8.62	0.31	2.33	7.39
$t_C^* = 30$ nm	0.26	1.62	6.93	0.30	1.62	5.41

*The latter are obtained by including into the calculation a carbon contaminating film of variable thickness t_C^* ($t_C^* = 0$ means no contamination). "Grid downward" geometry, tilt angle = 20°. The Monte Carlo statistical errors have not been reported, being negligible.

Table 6. Experimental and MC–Generated Intensity Ratios $I(\mathrm{OK})/I(\mathrm{NiK})$, $I(\mathrm{OK})/I(\mathrm{CK})$, and $I(\mathrm{NiK})/I(\mathrm{CK})$*

Q cross section	Grid Upward					
	B-W			Powell		
Intensity ratios	$\frac{I(\mathrm{OK})}{I(\mathrm{NiK})}$	$\frac{I(\mathrm{OK})}{I(\mathrm{CK})}$	$\frac{I(\mathrm{NiK})}{I(\mathrm{CK})}$	$\frac{I(\mathrm{OK})}{I(\mathrm{NiK})}$	$\frac{I(\mathrm{OK})}{I(\mathrm{CK})}$	$\frac{I(\mathrm{NiK})}{I(\mathrm{CK})}$
Experimental	0.251 ± 0.005	0.99 ± 0.02	3.95 ± 0.05	0.251 ± 0.005	0.99 ± 0.02	3.95 ± 0.05
Monte Carlo						
$t_C^* = 0$ nm	0.27	3.08	11.40	0.32	3.08	9.74
$t_C^* = 10$ nm	0.26	1.96	7.64	0.30	1.96	6.53
$t_C^* = 20$ nm	0.24	1.41	5.78	0.28	1.41	4.94
$t_C^* = 30$ nm	0.23	1.08	4.65	0.27	1.08	3.98

*The latter are obtained by including into the calculation a carbon contaminating film of variable thickness t_C^* ($t_C^* = 0$ means no contamination). "Grid upward" geometry, tilt angle = 20°. The Monte Carlo statistical errors have not been reported, being negligible.

sensible variation in the C_O and t values. We performed simulations by varying the NiO film thickness. From the results (not reported here), it appeared that to obtain the agreement between the experimental and the computed ratios $I(\mathrm{OK})/I(\mathrm{CK})$ and $I(\mathrm{NiK})/I(\mathrm{CK})$, the NiO film should be no thicker than about 30 nm, which is unrealistic.

A plausible conjecture is the presence of a carbon contamination on the sample surface. To take this into account, we simulated a geometry in which, besides considering both grid locations (downward and upward), there is a further carbon film on the sample surface, with thickness t_C^* ranging from 10 to 30 nm. Accordingly, new sets of Monte Carlo data were generated.

In Table 5 are reported the Monte Carlo–generated intensities ratios $I(\mathrm{OK})/I(\mathrm{NiK})$, $I(\mathrm{OK})/I(\mathrm{CK})$, and $I(\mathrm{NiK})/I(\mathrm{CK})$ compared with the experimental ones, by varying the thickness of the carbon contaminating film t_C^* in the "grid downward" geometry.

The results refer to a 20° tilt angle; however, a similar trend is found for both 10° and 15°. With t_C^* about 20 nm, the agreement between the Monte Carlo intensity ratios and the experimental ratio is satisfactory for both cross sections. Note that the $I(\mathrm{OK})/I(\mathrm{CK})$ ratios are the same (up to two decimals) for both cross sections.

Let us now consider the geometry with the "grid upward." In this case the sample is formed by a carbon film with thickness $t_C^* = 10$, 20, and 30 nm on the NiO film, which adds to the 20 nm carbon layer of the sample. Table 6 shows the Monte Carlo intensy ratios $I(\mathrm{OK})/I(\mathrm{NiK})$, $I(\mathrm{OK})/I(\mathrm{CK})$, and $I(\mathrm{NiK})/I(\mathrm{CK})$, obtained by varying the thickness of the carbon contamination t_C^* in the "grid upward" geometry, for a 20° tilt angle, compared with the experimental ones. In this case the agreement is still satisfactory around $t_C^* = 20$ nm, however for the Powell section, it is better for $t_C^* = 30$ nm. By applying the "2 tilt-angle" method, while taking into account the carbon contaminat-

ing film on the surface, we obtain in the "grid downward" geometry the results reported in Table 4. Notably with $t_C^* = 20$ nm, the agreement with the certified data is reached for both the cross sections. In any case, even for $t_C^* = 10$ nm and $t_C^* = 30$ nm, the agreement is fair.

In the "grid upward" geometry, the "2 tilt-angle" method, taking into account the carbon contamination on the surface, gives the results reported in Table 4. Even in this geometry, agreement is achieved for both cross sections by considering the presence of a contaminating carbon film with a thickness of about 20–30 nm.

Discussion

The Monte Carlo method applied to the experimental spectra taken on the investigated sample yields a composition of the NiO film in good agreement with the certified one, if the carbon support film is neglected.

However, if one takes into consideration in the Monte Carlo calculations all the different intensity ratios [i.e., $I(\mathrm{OK})/I(\mathrm{CK})$ and $I(\mathrm{NiK})/I(\mathrm{CK})$, in addition to $I(\mathrm{OK})/I(\mathrm{NiK})$], a clear disagreement between experimental and computed values is found. To remove this discrepancy, the solution is not just to assume a small variation in NiO composition and thickness of the NiO/C bilayer. We performed simulations by varying C_O in the range 40–60 at.% and t in the 30–80 nm range. The results have shown that in such ranges no agreement between experimental and computed values can be reached; clearly, exploring values outside this interval would make no sense.

The experimental intensity ratios come into agreement with the simulated ones only if the presence of a carbon contamination layer is assumed. It is plausible that such a layer would form as a thin film in our experimental conditions, despite the use of a LN2-anticontamination during the spectral acquisitions; probably, the use of spot sizes larger than the 1 nm beam employed for this work also could help in reducing this effect. Two important points emerge from our work: (1) a carbon thickness of about 20 nm is enough to ensure the agreement between the simulated and the experimental intensity ratios; (2) the agreement is verified by inserting this layer into the computer model for both the "grid downward" and "grid upward" geometries.

A further confirmation of our findings is given by two additional considerations. The first is experimental in character and concerns the application of the "2-tilt angle" method: the agreement between simulations and experiments does not appreciably change if two different coupled angles are employed (10–20° or 15–20°). The second point is more theoretical and has to do with the chosen equation for the ionization cross sections Q: we have investigated the effect of exchanging the Powell cross section with the one by Bethe (1930) (in the relativistic form proposed by Williams, 1933) and found composition and thickness values in mutual agreement, both for the "2-tilt angle" (single intensity ratio) method and the comparison between the two sets of the three intensity ratios (Tables 4–6).

Finally, this work quantitatively shows to what extent the position of the carbon supporting layer (upward or downward) affects the film composition. In quantitative thin film X-ray microanalysis, this effect cannot be neglected, especially when light elements are present (oxygen in this case).

Conclusions

The application of our Monte Carlo method to the quantitative X-ray microanalysis of a commercial, certified, 55 nm thick NiO film, deposited on a 20 nm carbon layer allows correct results to be obtained by Monte Carlo not only in terms of the Ni and O concentrations, but also of the thickness of carbon layer(s). The Monte Carlo approach can not only take into account the carbon layer, whatever its position in the microscope (upward or downward), but it can also ascertain the presence of a contamination built up during the acquisition of the X-ray spectra. In fact, it has been found that, if all the three ratios $I(\mathrm{NiK})/I(\mathrm{OK})$, $I(\mathrm{NiK})/I(\mathrm{CK})$, and $I(\mathrm{OK})/I(\mathrm{CK})$ are taken into account, Monte Carlo simulations of the experimental spectra allows the user to infer the presence of a contaminating carbon film on the sample surface. Finally, the more general case of X-ray microanalysis of electron transparent bilayers and triple layers consisting of different materials and including light elements can be effectively treated by the Monte Carlo–based methodology reported in this work.

Acknowledgments

This work has been partially supported by the Italian Ministry for Education, University and Research (MIUR 60% and MIUR 40% funds).

References

Armigliato, A. (1999). Thin film X-ray microanalysis with the analytical electron microscope. *J Anal At Spectrom* **14**, 413–418.

Armigliato, A. & Rosa, R. (1990). Simultaneous determination of composition and thickness of thin films by X-ray microanalysis at 300 kV and Monte Carlo simulation. *Ultramicroscopy* **32**, 127–136.

Bethe, H.A. (1930). Zur Theorie des Durchgangs Schneller Korpuskolarstrahlen Durch Materie. *Ann Phys* **5**, 325–400.

Cliff, G. & Lorimer, G. (1975). The quantitative analysis of thin films. *J Microsc* **103**, 203–207.

Egerton, R.F. (1996). *Electron Energy-Loss Spectroscopy in the Electron Microscope*, 2nd ed. New York: Plenum Press.

Egerton, R.F. & Cheng, S.C. (1994). Characterization of an analytical electron microscope with a NiO test specimen. *Ultramicroscopy* **55**, 43–54.

Horita, Z., Ichitani, K., Sano, T. & Nemoto, M. (1989). Applicability of the differential X-ray absorption method to the determinations of foil thickness and local composition in the analytical electron microscope. *Phil Mag A* **59**, 939–952.

Horita, Z., Sano, T. & Nemoto, M. (1986). An extrapolation method for the determination of Cliff-Lorimer k_{AB} factors at zero foil thickness. *J Microsc* **143**, 215–231.

Krause, M.O. (1979). Atomic radiative and radiationless yields for K and L shells. *J Phys Chem Ref Data* **8**, 307–327.

Pouchou, J.L. & Pichoir, F. (1991). Quantitative analysis of homogeneous or stratified microvolumes applying the model "PAP." In *Electron Probe Quantitation*, Heinrich, K.F.J. & Newbury, D.E. (Eds.), pp. 31–75. New York: Plenum Press.

Powell, C.J. (1976). Cross sections for ionization of inner shell electrons by electrons. *Rev Mod Phys A* **48**, 33–47.

Rosa, R. & Armigliato, A. (1989). Monte-Carlo simulation of thin film X-ray microanalysis at high energies. *X-ray Spectrom* **18**, 19–23.

Schreiber, T.P. & Wims, A.M. (1982). Relative intensity factors for K, L and M shell X-ray lines. *X-ray Spectrom* **11**, 42–45.

Veigele, W.M.J. (1973). Photon cross sections from 0.1 keV to 1 MeV for elements $Z = 1$ to $Z = 94$. *Atom Data Tables* **5**, 51–111.

Watanabe, M. & Williams, D.B. (2006). The quantitative analysis of thin specimens: A review of progress from the Cliff-Lorimer to the new ζ-factor methods. *J Microsc* **221**, 89–109.

Westwood, A.D., Michael, J.R. & Notis, M.R. (1992). Experimental determination of light-element *k*-factors using the extrapolation technique: Oxygen segregation in aluminium nitride. *J Microsc* **167**, 287–302.

Williams, E.J. (1933). Applications of the method of impact parameter in collisions. *Proc Roy Soc A* **139**, 163–186.